Galvanic coupling between copper and aluminium in a thin-layer cell

Christine Blanc [a], Nadine Pébère [a], Bernard Tribollet [b], Vincent Vivier [b,*]

[a] Université de Toulouse, CIRIMAT, UPS/INPT/CNRS, ENSIACET, 4 Allée Émile Monso, BP 44362, 31432 Toulouse Cedex 04, France
[b] Laboratoire Interfaces et Systèmes Électrochimiques, UPR 15 du CNRS, Université Pierre et Marie Curie, 4 Place Jussieu, CP 133, 75252 Paris Cedex 05, France

A B S T R A C T

The Al/Cu coupling was investigated in a thin-layer cell formed by a large Cu electrode and an Al microelectrode embedded in an insulator placed above the Cu electrode. By using a scanning electrochemical microscope (SECM) the thickness of the thin layer was perfectly controlled with a precision in the micrometer range. A copper deposit on an electrochemical quartz crystal microbalance (EQCM) was also used as SECM substrate to quantify the copper dissolution rate. It was shown that such an experimental set-up allows to mimic the galvanic corrosion of intermetallic particles embedded in the aluminium matrix of the 2XXX series aluminium alloys. The combination of the SECM and the EQCM permitted the evaluation of the corrosion rate of copper at the corrosion potential of the 2024 Al alloy, whereas cyclic voltammetry performed on the SECM tip indicated the enrichment in Cu^{2+} ions in the thin electrolyte layer.

Keywords:
A. Aluminium
A. Copper
A. Alloy

1. Introduction

In a previous study [1], a simple system consisting of a pure aluminium–pure copper couple was considered to understand the corrosion phenomena associated with copper-rich intermetallics in aluminium alloys. During immersion of the Al–Cu disk electrode in an aqueous electrolyte (10^{-3} M Na_2SO_4), aluminium is the anode and is in the passive state while copper is polarized cathodically. After 24 h of immersion, the formation of a copper deposit on the Al electrode, which is similarly observed during corrosion on commercial copper-rich aluminium alloys [2–5], was clearly shown. This phenomenon was explained by the formation of an occluded zone at the Al–Cu interface, in which the local chemical reactions enable copper corrosion.

The aim of the present study is to verify that the corrosion of a copper electrode can occur even though it is polarized cathodically at the corrosion potential of the Al/Cu couple by using a thin-layer cell in order to model the occluded zone. The use of a scanning electrochemical microscope [6,7] allowed the thin-layer cell dimension, i.e., the thickness of the thin layer, to be precisely controlled in the micrometer range. An electrochemical quartz crystal microbalance was used to quantify the copper dissolution rate.

2. Experimental

2.1. SECM–EQCM set-up

All experiments were performed with a home-made SECM set-up schematized in Fig. 1A. It consisted of a 3-axis positioning system (VP-25XA, Newport) driven by a motion encoder (ESP300, Newport) allowing a spatial resolution of 100 nm in the three directions. Electrochemical measurements were performed with a home-made bi-potentiostat coupled with a low noise current-to-voltage converter (Femto DLPCA 200) and controlled by a multifunction data acquisition card (National Instrument).

The electrochemical quartz crystal microbalance (EQCM) equipment was also a home-made device. The EQCM measured the change in the resonance frequency of a 9 MHz AT-cut quartz crystal (CQE, Troyes, France) resulting from the change in the mass of the electrode exposed to the solution. The two gold electrodes, deposited on the opposite faces of the quartz crystal, allowed the resonator to be electrically connected to an oscillator circuit. The software controlling the overall experiment was developed under Labview© environment for simultaneous experiments with SECM and EQCM techniques [8,9].

2.2. Electrode preparation and chemicals

For the EQCM measurements, copper was deposited on one side of the gold electrode from a 0.5 M copper sulfate electrolyte in 0.5 M sulfuric acid with a galvanostat. Thicknesses of the copper deposits (from 2 to 5 μm) were evaluated from charge exchanged during the reduction process assuming a 100% current yield for a 2-electron transfer reduction reaction. The copper deposits were homogeneous without any crack.

The SECM experiments were performed using a Cu rod (99.99% – Goodfellow) as the working electrode. A 5 mm long Cu cylinder was insulated with a cataphoretic paint and then molded in an epoxy resin, forming a conventional Cu disk electrode (8 mm in

Corresponding author. Tel.: +33 1 4427 4158; fax: +33 1 4427 4074.
E-mail address: vincent.vivier@upmc.fr (V. Vivier).

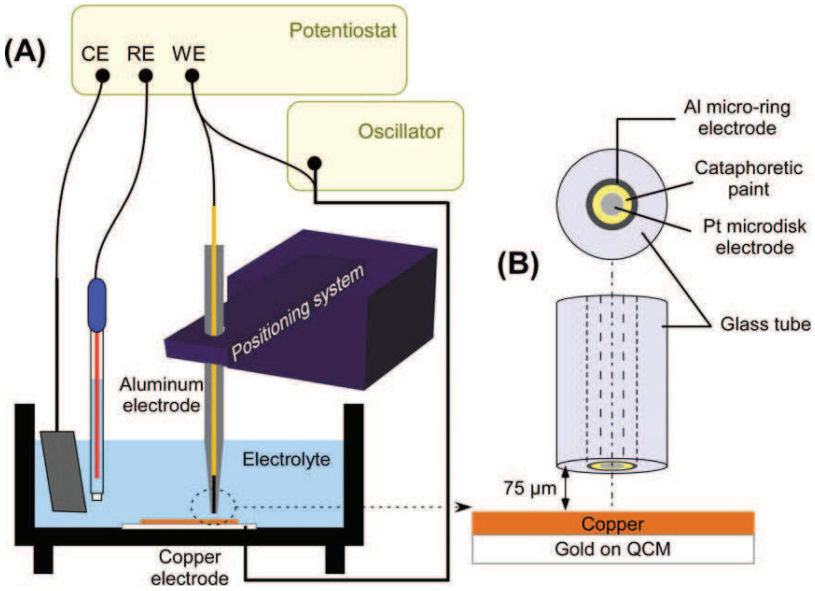

Fig. 1. Experimental set-up used for studying the galvanic coupling between pure Al and pure Cu (A), and magnification of the thin-layer cell formed by the Al–Pt ring-disk microelectrode and the copper electrode (B).

diameter). The anodic behaviour of bulk Cu was similar to the behaviour of the electrolytic deposited layer.

A specific SECM tip was developed, allowing cupric ions to be detected during the corrosion process. Formally, it consisted of an Al–Pt ring-disk microelectrode as shown in Fig. 1B. A 50 µm in diameter Pt wire (Goodfellow) was insulated using a cataphoretic paint. It was then inserted in an Al tube (inner diameter 300 µm, outer diameter 600 µm) and sealed with an epoxy resin. The lateral part of the Al tube was also insulated with the cataphoretic paint prior to the sealing of the assembly in a glass capillary, the external diameter of which was 1 mm. When the tip was brought in the close vicinity of the copper substrate (see below), it formed a cylindrical thin-layer cell of radius r_g (the total radius of the ring-disk microprobe) and of thickness z equal to the distance between the probe and the substrate.

The electrolyte was a 10 mM Na_2SO_4 solution prepared with analytical grade chemicals used as received in twice-distilled water at room temperature. Electrochemical experiments were carried out with a Pt gauze as counter-electrode and a saturated sulfate electrode (SSE) as reference electrode (E = 0.655 V/NHE).

2.3. Electrode positioning and control of the thin-layer cell thickness

In a conventional SECM experiment, the use of a redox mediator allows the distance between the tip and the substrate to be controlled accurately by performing approach curves in the feedback mode [10,11]. In this study, copper and aluminium electrodes are used together in solution. Thus, the addition of a redox moiety is a significant drawback since it can significantly modify the corrosion potential of the system. However, tip-to-substrate distance can also be controlled without redox mediator, e.g., by measurement of shear forces [12,13], high-frequency ac measurements [14,15], or the combined use of AFM–SECM [16,17]. For experiments performed on the Cu rod, high-frequency impedance measurement was advantageously used, since it was previously shown that the approach curves performed in ac-mode were similar to those obtained in the feedback mode in the presence of a redox mediator [15,18]. For this measurement, a 50 mV sine wave perturbation was superimposed to the dc-potential of the platinum microelectrode, and a home-made analog device described elsewhere was used for monitoring the modulus of the impedance variations [15]. For experiments involving the simultaneous use of SECM and EQCM, the quartz frequency variations were used for positioning the tip at a given distance of the substrate with an accuracy of 100 nm corresponding to the resolution of the positioning system used in this study [8,9]. First, the tip was brought into contact with the substrate at low scan rate, hence making possible to determine the vertical position z = 0. Then, the probe was withdrawn at the required tip-to-substrate distance.

2.4. Calibration of the electrochemical quartz crystal microbalance for the study of a local event

The mass variation of the thin layer of copper deposited on the quartz crystal microbalance was evaluated from the frequency variations through the Sauerbrey's equation:

$$\Delta f = -C_f \Delta m \quad (1)$$

where Δf is the frequency variation, Δm is the mass variation, and C_f is the integral sensitivity. From this law, a frequency variation of 1 Hz corresponds to a mass variation of 1.1 ng for a quartz resonator of 9 MHz. This relationship applies for the overall electrode surface. Sauerbrey's law remains applicable for a local event, however, Sauerbrey's coefficient becomes dependent on the radial position of the local event on the quartz crystal microbalance [19]. Thus, in Eq. (1), the coefficient C_f must be replaced by the differential mass sensitivity, which is position dependent. The minimum differential mass sensitivity is obtained at the electrode edge, whereas the maximum value is at the centre, and its distribution follows a Gaussian curve as a first approximation [19,20]. The local quartz sensitivity was evaluated from quartz characteristics, numerical calculations and from calibration experiments. This was achieved by performing several copper deposits of controlled size on various locations on the electrode of the EQCM. An image analysis allows the location of copper deposits to be determined with a good approximation. The radial sensitivity of the quartz is evaluated from the quantitative analysis of both current and frequency variations, and the results were then fitted using a Gaussian curve. The thin-layer cell was thus formed as close as possible to the electrode centre to get a larger sensitivity for the mass variation measurements

[8,9,20], and the exact position of the local event was determined post-mortem by optical observation of the sample. This procedure allows the actual differential mass sensitivity coefficient to be determined for the evaluation of the mass variation from frequency variation measurements.

3. Results and discussion

Fig. 2 shows the current response to a potential step applied at the copper electrode from −0.310 V/SSE (corresponding to the corrosion potential of a pure copper electrode) down to −0.745 V/SSE (corresponding to the corrosion potential of the Al/Cu couple measured in a preliminary experiment). This experiment was performed in a thin-layer cell formed by the ring-disk microprobe, the copper electrode, and a 10 mM Na_2SO_4 solution film between the electrodes. The thin-layer thickness was set at 75 μm. During the whole experiment, the Al ring electrode was left at its free potential and was not connected to any external electrical device. After a sharp step change at the outset, the current tends towards −0.7 μA. This current value was ascribed to the oxygen reduction reaction occurring on the copper surface. After 2 h of immersion, no copper corrosion could be observed. Similar experiments were performed by varying the tip-to-substrate distance in the range of 20–500 μm, and by extending the immersion time up to 4 h. In any of these cases, no corrosion of the copper electrode was shown.

Fig. 3a shows the simultaneous evolution of the corrosion potential (left-hand scale) and of the frequency variation (right-hand scale) of the copper electrode before and after electrical connection of the Cu and Al electrodes. Before connection (t < 60 min) the potential of the Cu electrode remained stable and no significant frequency variations were noticed. When Al and Cu electrodes were connected, a sharp variation of the potential was shown and was accompanied by a mass decrease (frequency increase). After one hour connection, the potential of the system tends towards −0.760 V/SSE, which is similar to that of the Al/Cu couple. The mass variations were quite linear and, from the slope of the curve, the copper dissolution rate was determined at about 150 ng h^{-1}.

Fig. 3b shows the evolution of corrosion potential and mass variation of the copper electrode when Al and Cu electrodes were initially connected for one hour and then disconnected. The distance between the Cu and the Al electrode was also 75 μm. During the first 60 min, when the electrodes were connected, the corrosion potential of the system remained constant at −0.770 V/SSE, and

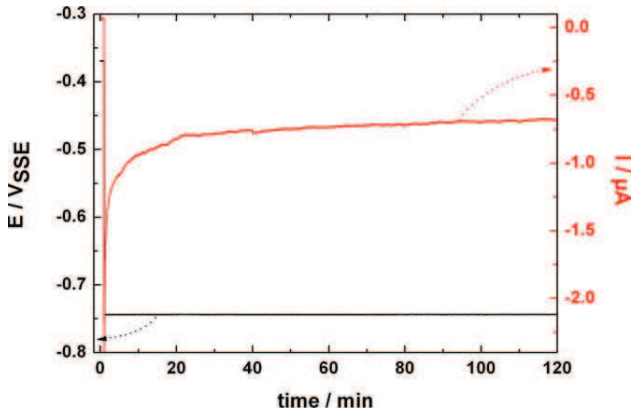

Fig. 2. Current response to a potential step of a copper electrode in a thin-layer cell (d = 75 μm) in a 10 mM Na_2SO_4 solution. Aluminium and copper electrodes were not connected together, i.e., only the copper electrode was biased (at a potential corresponding to the corrosion potential of the Al/Cu couple) whereas the potential of Al electrode was set at its free potential.

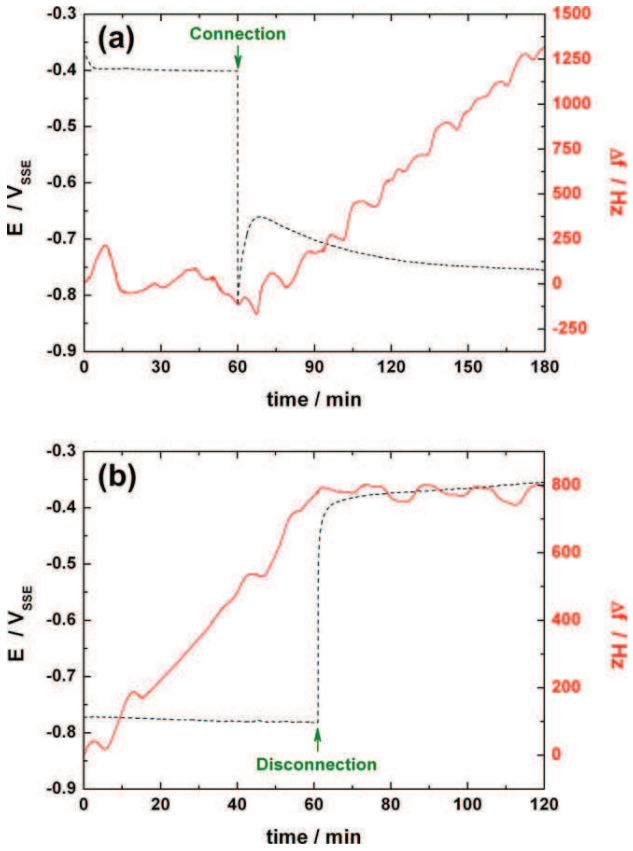

Fig. 3. Evolution of the corrosion potential of a copper electrode in a thin-layer cell (d = 75 μm) in a 10 mM Na_2SO_4 solution and frequency variations. (a) Aluminium and copper electrodes were connected together after one hour immersion; (b) aluminium and copper electrodes were disconnected after one hour of connection.

the dissolution rate of Cu was the same as in Fig. 3a, indicating a fairly good reproducibility of the experiment. When the two electrodes were disconnected, the frequency stopped to increase and remained constant whereas the potential of the copper electrode rapidly evolved towards more positive values.

Fig. 4 shows a SEM image of the copper electrode after 180 min of immersion in 10 mM Na_2SO_4 solution in the thin-layer cell and connected with the Al electrode. The mark due to the local reactivity in the confined volume delimited by the thin-layer cell is visible as a light shadow in Fig. 4. Two specific areas of about 40 μm in diameter each and separated by 100 μm correspond to localized sites of corrosion where copper dissolved. A careful examination of the sample surface after each experiment indicated that reactive sites were located inside the thin layer only. Cu dissolution can result in either pitting or blistering [21]. Blistering can be seen as an intermediary step to the pit formation, i.e., a confined domain with a protective cap in which corrosion propagates (Fig. 4). Mankowski et al. [21] have shown that sulfate ions are responsible for pitting phenomena on copper and the pit morphology was always hemispherical with the presence of caps of corrosion products with a duplex structure (cupric hydroxide and brochantite – $Cu_4SO_4(OH)_6$). Outside the thin-layer cell, the copper electrode appears unattacked, indicating that copper dissolution only occurs inside the domain formed by the thin layer.

From the corrosion rate evaluated with the EQCM experiments (150 ng h^{-1}) and from the copper density (ρ = 8.92 g cm^{-3}), one hour corrosion leads to the dissolution of 1.7×10^{-8} cm^3 of Cu (corresponding to 2.4 nmol). Assuming a 50 μm circular active area, the depth of the hole should be in the range of 8.5 μm, which

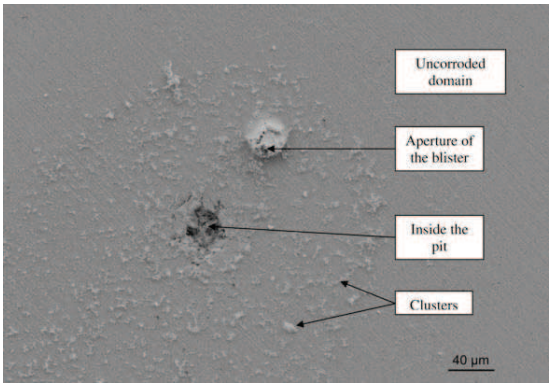

Fig. 4. SEM image of the copper electrode after corrosion (180 min immersion) in 10 mM Na_2SO_4 solution in a thin-layer cell. Aluminium and copper electrodes were connected together.

is in quite good agreement with a rough approximation obtained from SEM observations performed on a tilted sample.

Results of EDS analysis performed on various locations of the copper electrode surface are reported in Table 1. At the aperture of the blister and inside the pit (see Fig. 4), the atomic ratios of each element were similar and matched the formation of both copper oxide (CuO) and aluminium oxide (Al_2O_3). Moreover, many clusters of few micrometers or less in diameter, identified by EDS analysis as Al_2O_3 deposits, were observed on the Cu surface outside the pits (Fig. 4). The presence of Al_2O_3 should be ascribed to the dissolution of the Al electrode in the thin layer. The formation of the aluminium oxide points out that the pH in the thin layer should be larger than 9 for allowing the Al dissolution [1,22].

Fig. 5 shows reference cyclic voltammograms (CV), with the cupric ion concentration as a parameter (between 4 and 24 mM), obtained with a 50 µm in diameter Pt microelectrode in 10 mM Na_2SO_4 solution. The cathodic reaction corresponds to the deposition of copper at the electrode, whereas the oxidation peak corresponds to the dissolution of the copper deposit. These curves exhibit the possibility of copper ion detection during the dissolution step, as already described in the literature [23].

Fig. 6 shows the cyclic voltammograms obtained with the Al–Pt ring-disk electrode in the thin-layer cell. Copper and aluminium were connected after 5 min of immersion (Fig. 6a) and 30 min (Fig. 6b). For comparison, some curves from Fig. 5 are also reported. After 5 min, the amount of copper ions was similar to that obtained in the 4.1 mM reference solution. After 30 min, it was shown that the concentration was about four times larger. From these concentrations, it was possible to evaluate the amount of dissolved copper in the thin-layer cell at about 0.9 nmol which compares with the value of 1 nmol determined from EQCM measurements (Fig. 3). These results clearly show that Cu dissolves. The dissolved oxygen inside the thin-layer cell is rapidly consumed [24], which should be responsible to local pH variations, but the true composition of the solution inside the thin layer is not known. Conversely, at such a negative potential, the electrochemical reaction occurring on Cu outside the thin-layer cell is the oxygen reduction reaction.

Table 1
Elemental analysis performed on various locations of a corroded Cu electrode (see Fig. 4).

Element (at.%)	O	Al	Cu	S	Total
Inside the pit	48.6	7.2	41.1	3.1	100
Aperture of the blister	50	12.3	35.8	1.9	100
Deposits	43.8	37.9	17.4	0.9	100
Uncorroded area	5.2	2.2	92.6	–	100

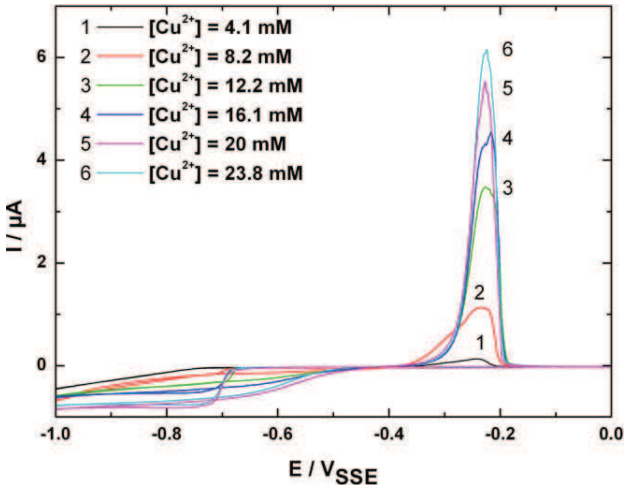

Fig. 5. Cyclic voltammograms performed on a 50 µm in diameter Pt microelectrode in 10 mM Na_2SO_4 supporting electrolyte with the concentration of cupric ion as a parameter. Scan rate: 50 mV s^{-1}.

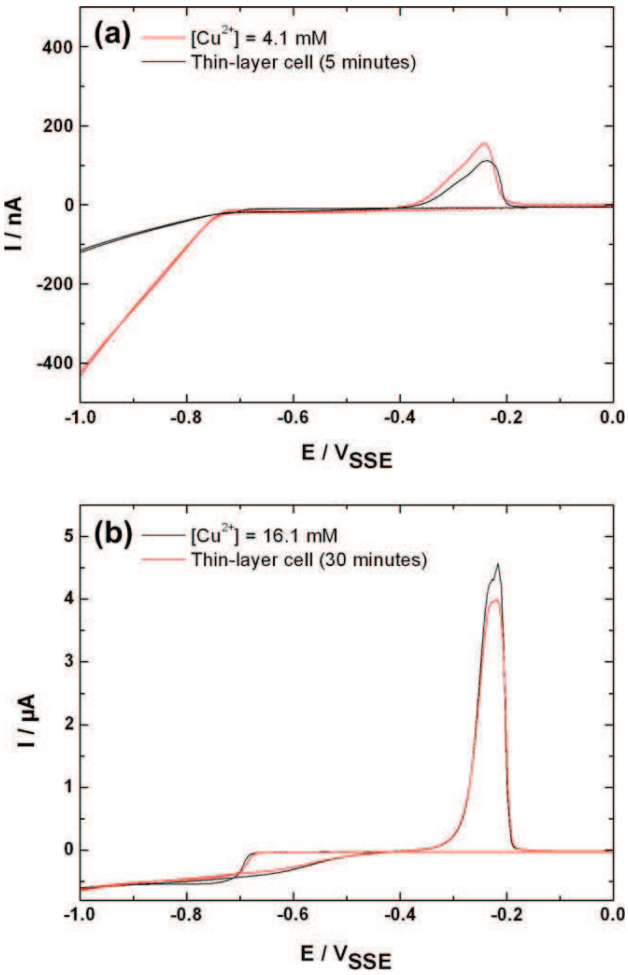

Fig. 6. Cyclic voltammograms performed on a 50 µm in diameter Pt microelectrode in 10 mM Na_2SO_4 in the thin-layer cell after 5 min (a), and 30 min (b) of immersion. Scan rate: 50 mV s^{-1}.

In contrast, no dissolved copper was detected (both by CV and EQCM experiments) if Al and Cu were not connected together, or if the distance between the two electrodes was larger than 150 μm. However, this value is to handle with care since another parameter that has not been investigated in this work is the surface area ratio of the two electrodes that can play a significant role in the galvanic coupling.

4. Conclusions

The galvanic coupling of the Al/Cu system was studied using the combination of the SECM and the EQCM. The results obtained indisputably show the copper dissolution even if the potential of the system is negative with respect to the corrosion potential of pure copper. It was shown that the Al can also dissolve, which was observed by the presence of alumina clusters on the Cu electrode. In the absence of the Al electrode, or when the distance between the two metals was too large, no copper corrosion was shown. Thus, it can be concluded that the chemistry in the thin-layer cell should play (at least on a local scale) a significant role.

References

[1] J.B. Jorcin, C. Blanc, N. Pebere, B. Tribollet, V. Vivier, J. Electrochem. Soc. 155 (2008) C46–C51.
[2] C. Blanc, B. Lavelle, G. Mankowski, Corros. Sci. 39 (1997) 495.
[3] C. Blanc, S. Gastaud, G. Mankowski, J. Electrochem. Soc. 150 (2003) B396.
[4] T. Suter, R. Alkire, J. Electrochem. Soc. 148 (2001) B36.
[5] Y. Yoon, R.G. Buchheit, J. Electrochem. Soc. 153 (2006) B151.
[6] A.J. Bard, F.-R.F. Fan, J. Kwak, O. Lev, Anal. Chem. 61 (1989) 132–138.
[7] J.V. Macpherson, P.R. Unwin, J. Phys. Chem. 99 (1995) 14824–14831.
[8] C. Gabrielli, S. Joiret, M. Keddam, H. Perrot, N. Portail, P. Rousseau, V. Vivier, J. Electrochem. Soc. 153 (2006) B68–B74.
[9] C. Gabrielli, S. Joiret, M. Keddam, H. Perrot, N. Portail, P. Rousseau, V. Vivier, Electrochim. Acta 52 (2007) 7706–7714.
[10] A.J. Bard, F.-R.F. Fan, M.V. Mirkin, in: I. Rubinstein (Ed.), Physical Electrochemistry. Principles, Methods, and Applications, Marcel Dekker, Inc., New York, 1995 (Chapter 5).
[11] J. Kwak, A.J. Bard, Anal. Chem. 61 (1989) 1221–1227.
[12] B.B. Katemann, A. Schulte, W. Schuhmann, Electroanalysis 16 (2004) 60–65.
[13] A. Hengstenberg, C. Kranz, W. Schuhmann, Chem. Euro. J. 6 (2000) 1547–1554.
[14] B.R. Horrocks, M.V. Mirkin, D.T. Pierce, A.J. Bard, G. Nagy, K. Toth, Anal. Chem. 65 (1993) 1213–1224.
[15] C. Gabrielli, F. Huet, M. Keddam, P. Rousseau, V. Vivier, J. Phys. Chem. B 108 (2004) 11620–11626.
[16] J.V. Macpherson, Encyclopedia Electrochem. 3 (2003) 415–443.
[17] A. Davoodi, J. Pan, C. Leygraf, S. Norgren, Appl. Surf. Sci. 252 (2006) 5499–5503.
[18] M.A. Alpuche-Aviles, D.O. Wipf, Anal. Chem. 73 (2001) 4873–4881.
[19] A.C. Hillier, M.D. Ward, Anal. Chem. 64 (1992) 2539–2554.
[20] C. Hess, K. Borgwarth, J. Heinze, Electrochim. Acta 45 (2000) 3725–3736.
[21] G. Mankowski, J.P. Duthil, A. Giusti, Corros. Sci. 39 (1997) 27–42.
[22] M. Pourbaix, Atlas of Electrochemical Equilibria in Aqueous Solutions, Pergamon, New York, 1966.
[23] C. Gabrielli, E. Ostermann, H. Perrot, V. Vivier, L. Beitone, C. Mace, Electrochem. Commun. 7 (2005) 962–968.
[24] E. Remita, D. Boughrara, B. Tribollet, V. Vivier, E. Sutter, F. Ropital, J. Kittel, J. Phys. Chem. C 112 (2008) 4626.